Final report

“Coupled homeostasis of membrane lipids and stress proteins”

The present final report has two parts. In the first part we show our progress we made on sHsp deletion *E. coli* mutant cells concerning the role of these proteins in membrane stability during heat stress.

Small heat shock proteins (sHsps) are ubiquitous molecular chaperones that are known to protect soluble proteins from thermal aggregation keeping them in a refolding competent state for subsequent recovery . However, findings suggest that sHsp of *E coli*, IbpA/B proteins may protect essential cellular components or compartments other than soluble proteins.

Here we show evidence that IbpA/B proteins, especially IbpA, are not just localized to membranes, but they could be involved in the immediate preservation of cell membrane integrity during extreme heat stress.

I.

Deletion of IbpAB alters membrane phenotype and cell survival

In this study we tested the potential role of IbpA/B proteins in the *E. coli* cellular membranes and followed how membrane alterations could influence cell viability. When intact, the *E. coli* outer membrane nearly excludes hydrophobic substances such as the lipophilic fluorescent probe NPN, however, once the outer membrane is destabilized, entry of NPN into the phospholipid bilayer results in marked fluorescence. We have shown that the outer membrane of cells went through an abrupt permeability transition at around 50 °C upon a short term (15 min) heat treatment, which showed a notable coincidence with the expression of *ibpA* and *ibpB* genes, detectable only above 48 °C (Fig.1A). Although uptake of the fluorescent dye still increased after the main transition indicating further possible damages of inner membranes cellular death was clearly correlated with the loss of the permeability barrier function of outer membrane (Fig. 1A)

Surprisingly, whereas outer membrane of ΔIbpAB cells appeared to be more permeable to the fluorescent probe the rapid increase in NPN uptake was raised up to a higher temperature in ΔIbpAB cells (55 °C vs. 52 °C for WT cells), a phenomenon that was paralleled with an apparent heat tolerance of IbpAB deficient cells (Fig. 1B).

A

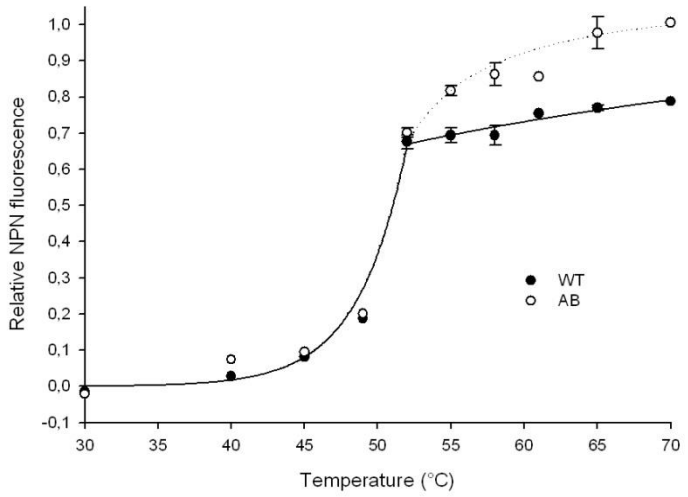

B

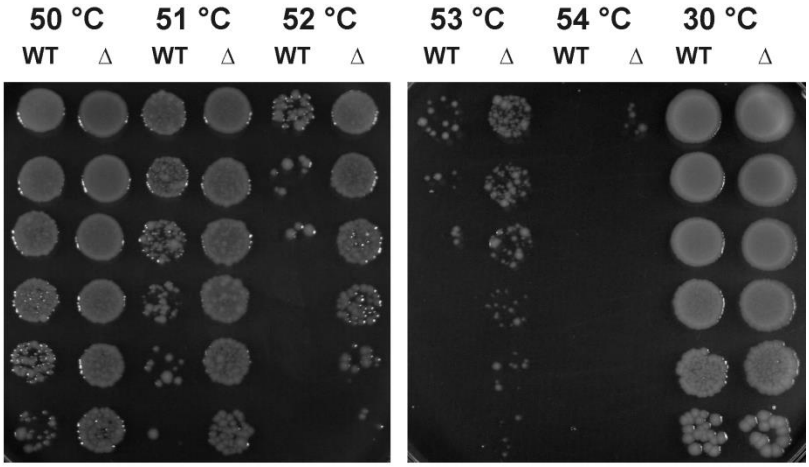

Figure 1.(A) *Permeability of cellular membranes. Cell membrane permeability of WT and IbpAB deficient (ΔIbpAB) cells exposed to different temperatures for 15 min was followed by measuring NPN fluorescence intensities. Data series were fitted and the WT plot (solid line) was compared to the normalized plot of ΔIbpAB cells (long dash line).* ***(B)*** *Viability of WT and ΔIbpAB cells. Ten-, five- or twofold serial dilutions were made of cells either left at 30 °C, incubated at 50, 51, 52 °C or 53, 54 °C for 15 min, respectively. Samples were plated on LB agar and incubated at 30 °C overnight.*

Exogenous sHsp production restores WT membrane phenotype

Supposing that IbpA/B proteins might affect cell membranes directly we expressed exogenous sHsps in ΔIbpAB cells to restore WT membrane phenotype. IbpA, IbpB and IbpAB proteins were expressed in ΔIbpAB cells to a similar extent to that produced in WT cells exposed to heat stress for 15 min, ensuring thereby a real comparison between replacement strains and WT cells (Fig. 2 Insert). While IbpB caused just little effect on the membrane phenotype of ΔIbpAB cells heterogenous expression of IbpA or IbpAB proteins resulted in a considerable restoration of WT membrane permeability at high temperatures as revealed by NPN fluorescence measurements. On the other hand, ΔIbpAB cells producing IbpA or IbpAB proteins already at 30 °C exhibited a strange increase in NPN uptake and showed an unusual shape of permeability transition, implying the possible membrane activity of these proteins at lower temperature, too.

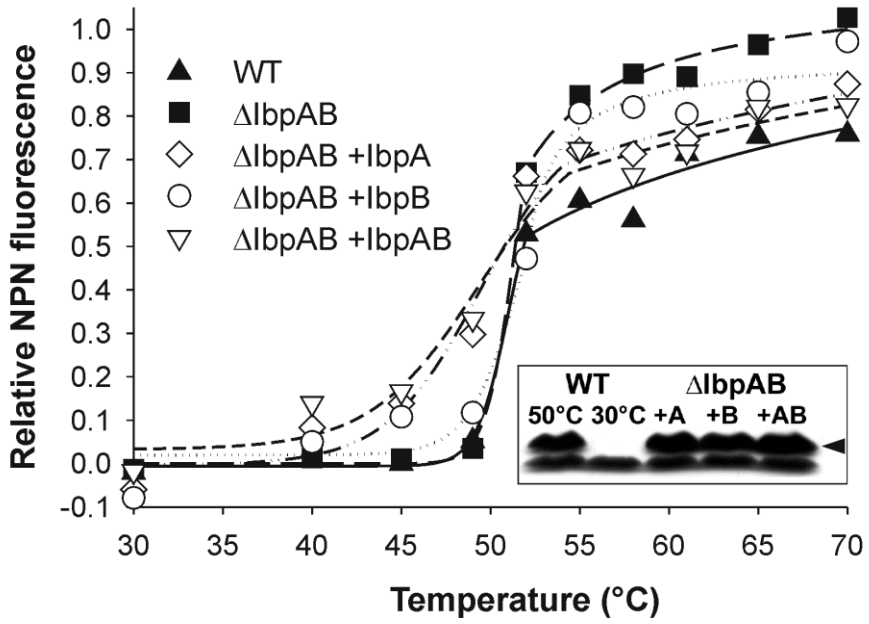

Figure 2. *Permeability of cellular membranes. Cell membrane permeability of WT, ΔIbpAB and IbpA-, IbpB- or IbpAB-expressing ΔIbpAB cells exposed to different temperatures for 15 min was followed by measuring NPN fluorescence intensities. Data series of WT, ΔIbpAB, ΔIbpAB +IbpA, ΔIbpAB +IbpB and ΔIbpAB +IbpAB cells were fitted and the plots, each of which was compared to the normalized plot of ΔIbpAB cells, are shown as solid, long dash, dash-dot-dot, dotted and short dash lines, respectively.* ***(Insert)*** *Immunoblotting analysis of IbpAB produced in WT cells kept at 30 °C (WT 30 °C) or heat-stressed at 50 °C for 15 min (WT 50 °C) and in ΔIbpAB cells that exogenously expressed IbpA (ΔIbpAB +A), IbpB (ΔIbpAB +B) or IbpAB (ΔIbpAB +AB). Band corresponding to IbpAB is indicated by arrowhead. IbpA/B proteins were not detectable in ΔIbpAB cells either kept at 30 °C or heat-stressed at 50 °C for 15 min (data not shown).*

It should be noted that empty and repressor vectors introduced into ΔIbpAB cells supplemented with the appropriate amounts of antibiotics and IPTG clearly did not influence the membrane permeability at high temperatures but slightly affected it at lower temperatures closely resembling that observed for IbpB-expressing ΔIbpAB cells below 50 °C (data not shown).

IbpA/B proteins rigidify membrane periphery

Similarly, while *E. coli* WT cells were faced with a short term heat exposure at 50 °C IbpA/B proteins were expressed and localized to the inner and especially to the outer membrane (Fig. 3A Insert).

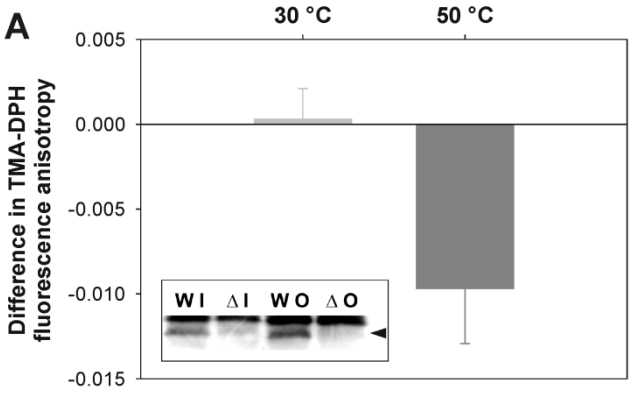

B

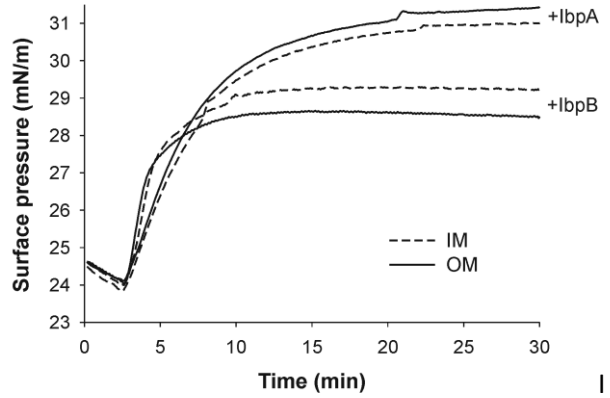

C

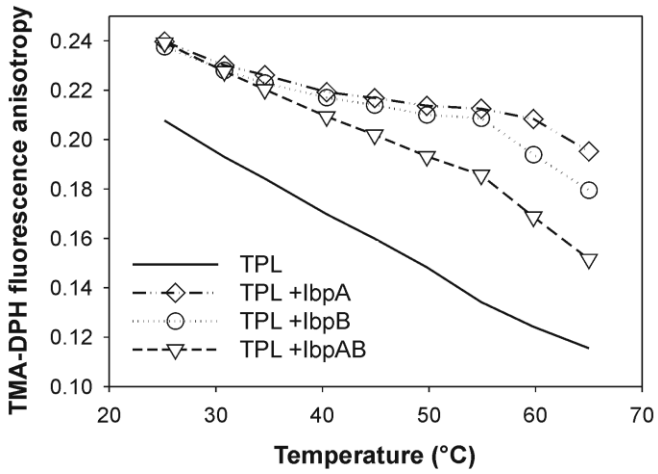

Figure 3 (A) *Fluidity of cell membrane periphery. Cell membrane fluidity at the head group region was characterized by determining TMA-DPH fluorescence anisotropy. Steady-state fluorescence anisotropy was measured at 30 or 50 °C, and the values of WT cells were subtracted from those of ΔIbpAB cells.* ***(Insert)*** *Immunoblotting analysis of inner (I) and outer (O) membrane fractions isolated from WT (W) or ΔIbpAB (□) cells heat-treated at 50 °C for 15 min. Band corresponding to IbpAB is indicated by arrowhead. IbpA/B proteins were not detectable in the membrane samples isolated from either WT or ΔIbpAB cells grown at 30 °C (data not shown).* ***(B)*** *Interaction of IbpA or IbpB with monomolecular lipid layers. IbpA or IbpB (6.8 µg/ml) was injected underneath monolayers of total polar lipids (TPL) isolated from inner (IM) or outer membranes (OM) of WT cells grown at 30 °C. Injection of proteins is indicated by arrowhead.* ***(C)*** *Fluidity of liposome membrane periphery. LUVs made of total polar lipids (TPL) (23 µg/ml) extracted from isolated outer membrane of WT cells grown at 30 °C were incubated with purified IbpA, IbpB or IbpAB proteins (15 µg/ml) at 20 °C, then TMA-DPH fluorescence anisotropy was measured at distinct temperatures as indicated.*

It should be noted that there were no sHsps detectable in either membranes or total lysate of *E. coli* cells grown at 30 °C (data not shown). Fluorescence anisotropy measured by applying the probe TMA-DPH located nearby the membrane surface is a good indicative of fluidity at the lipid head group region. Whereas the membrane physical state was apparently unaffected in ΔIbpAB cells at 30 °C, deletion of IbpAB resulted in significant fluidization at the membrane periphery at 50 °C as shown by TMA-DPH anisotropy measurements (Fig. 3A). Since membrane localization of IbpA/B proteins was correlated with an increase in membrane physical order *in vivo* we further tested the interaction of purified IbpA/B proteins with lipids isolated from WT cells *in vitro*.

Purified IbpA and IbpB proteins displayed a notable difference in their ability to interact with monomolecular lipid layers formed by total polar lipids isolated from either inner or outer membranes of WT cells (Fig. 3B).

IbpA, IbpB and the mixture of IbpA/B proteins interacted with liposomes and markedly decreased the fluidity of lipid membranes at the head group region. Moreover, IbpA and IbpB alone exerted more and more intense rigidifying effect with increasing temperatures up to even 55 and 60 °C, respectively. Interestingly, IbpAB proteins influenced fluidity of liposome membranes quite the same way as the sHsps did alone at lower temperatures but their effect was hardly affected by temperature variations (Fig. 3C).

Compensatory changes in the fatty acid region of ΔIbpAB cellular membranes

Deletion of *ibpAB* conferred heat resistance on the mutant cells (Fig. 1B). These findings suggested that removal of IbpAB may be accompanied with additional changes that could compensate the effects of the absence of these sHsps in mutant cells. Since deletion of *ibpAB* has been shown not to influence protein aggregation/ renaturation upon short term heat exposure we supposed that the apparent heat tolerance of ΔIbpAB cells might be related to the altered membrane phenotype. Among others changes in the lipid and fatty acid composition are known to have important function in the regulation of the physical state and phase behaviour of cellular membranes.

Intriguingly, inactivation of *ibpAB* raised the level of phospholypase A1 and the unsaturated vaccenic acid (18:1v) in cell membranes irrespective of heat conditions (data not shown and Table 1.). Accumulation of 18:1v is known to occur during cold acclimation at the expense of palmitic acid (16:0). This change in the fatty acid composition was, however, clearly distinguishable form that occured either in WT or in ΔIbpAB cells during cold/ heat acclimation and appeared to show a unique feature. In agreement with the lipid unsaturation, deletion of *ibpAB* was paralleled with the fluidization of membrane hydrophobic interior both at 30 and 50 °C as shown by DPH anisotropy measurements (Fig. 4A). Although sHsps are also known to influence the fatty acid region of membranes, IbpA/B proteins were not detectable in membranes isolated from cells grown at 30 °C and proved to hardly rigidify this region even at higher temperatures *in vitro* (data not shown).

	30 °C		50 °C	
	WT	**ΔIbpAB**	**WT**	**ΔIbpAB**
14:0	3.0 ±0.4	2.2 ±0.2	6.3 ±0.4	4.0 ±0.2
15:0	0.9 ±0.2	0.6 ±0.3	0.7 ±0.1	0.5 ±0.2
16:0	**28.0 ±2.4**	**26.0 ±1.6**	**32.4 ±0.6**	**31.3 ±1.2**
16:1	**31.3 ±1.3**	**31.2 ±0.3**	**31.8 ±1.3**	**28.1 ±1.1**
c17:0	2.5 ±0.5	2.0 ±0.2	1.8 ±0.2	2.0 ±1.4
18:0	1.7 ±1.2	1.3 ±0.2	1.0 ±0.2	1.3 ±0.3
18:1	0.5 ±0.3	0.3 ±0.1	0.4 ±0.2	0.5 ±0.2
18:1v	**31.7 ±1.5**	**36.3 ±1.4**	**24.6 ±1.0**	**31.4 ±0.8**
c19:0	0.8 ±0.4	0.3 ±0.2	0.9 ±0.1	0.8 ±0.2

Table 1. *Fatty acid composition of cell membrane phospholipids (mol/mol %). Lipids were isolated from WT and ΔIbpAB cells either kept at 30 °C or exposed to 50 °C for 15 min. Fatty acids identified are myristic acid (14:0); pentadecanoic acid (15:0); palmitic acid (16:0); palmitoleic acid (16:1); C_{17} cyclopropane acid (c17:0); stearic acid (18:0); oleic acid (18:1); vaccenic acid (18:1v) and sterculic acid (c19:0). Similar changes were detected in each of the lipid classes (data not shown).*

The crystal violet (CV) growth inhibition assay relies on membrane permeability/ phenotype differences. CV sensitivity at normal growth temperature has been shown to correlate with high temperature sensitivity. CV dissolved in LB agar plates revealed a notable difference between WT and ΔIbpAB cells with regards to their membrane-related viability. IbpAB deficient cells grown on CV plates displayed an increased viability under both normal and heat conditions (Fig. 4B). Given the correlation between the lipid unsaturation, increased membrane fluidity in the fatty acid region and CV sensitivity we proposed that such changes in the composition and physical state of membranes is involved in the aquired termotolerance of ΔIbpAB cells (Fig. 4C).

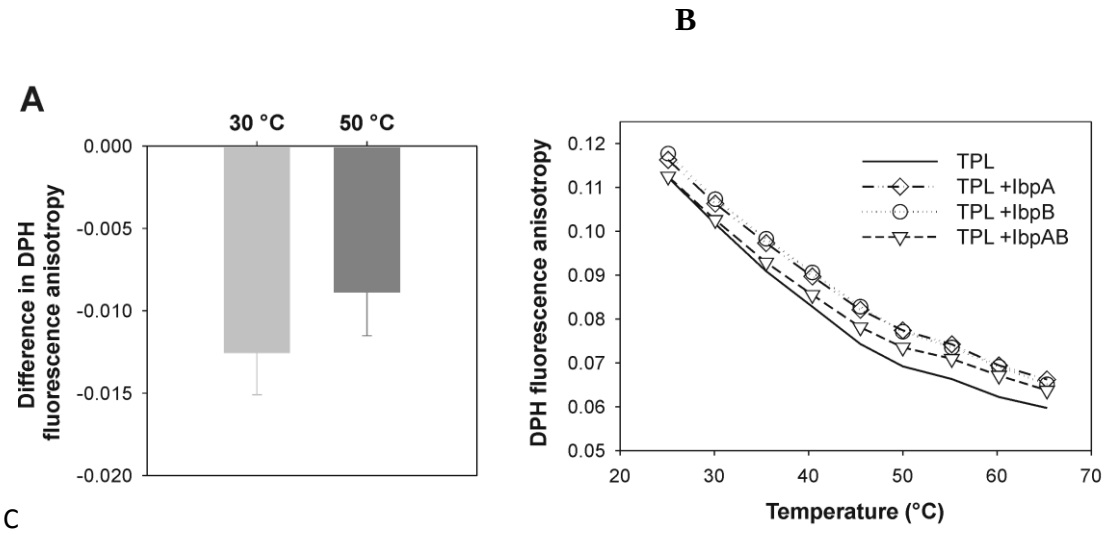

Figure 4. (A) Fluidity of hydrophobic interior of cell membranes. Cell membrane fluidity in the fatty acid *region was characterized by determining DPH fluorescence anisotropy. Steady-state fluorescence anisotropy was measured at 30 or 50 °C, and the values of WT cells were subtracted from those of ΔIbpAB cells.* ***(B)*** *Fluidity of hydrophobic interior of liposome membranes. LUVs made of total polar lipids (TPL) (23 µg/ml) extracted from isolated outer membrane of WT cells grown at 30 °C were incubated with purified IbpA, IbpB or IbpAB proteins (15 µg/ml) at 20 °C, then DPH fluorescence anisotropy was measured at distinct temperatures as indicated.* ***(C)*** *Membrane phenotype of WT and ΔIbpAB cells tested by crystal violet growth inhibition assay. Ten- and fivefold serial dilutions were made of cells either left at 30 °C or incubated at 50 °C for 15 min, respectively. Samples were plated on LB agar containing 2.5 µg/ml crystal violet and incubated at 30 °C overnight. See for comparison viability of WT and ΔIbpAB cells on normal LB agar plates (Fig. 1B).*

High throughput whole transcriptome analysis of wild-type and the IbpAB$^-$ cells

In order to find the basis of the unexpected phenotypes (heat resistance, changes in fatty acid composition) of IbpAB-deficient *E. coli* strain, we performed high throughput whole transcriptome analysis. Wild-type and the IbpAB$^-$ cells were grown at 30 °C and subjected to heat stress at 50 °C for 15 min, then total RNA were isolated. RNA-Seq analyses were carried out using 5500 Series Genetic Analyzer (Life Technologies).

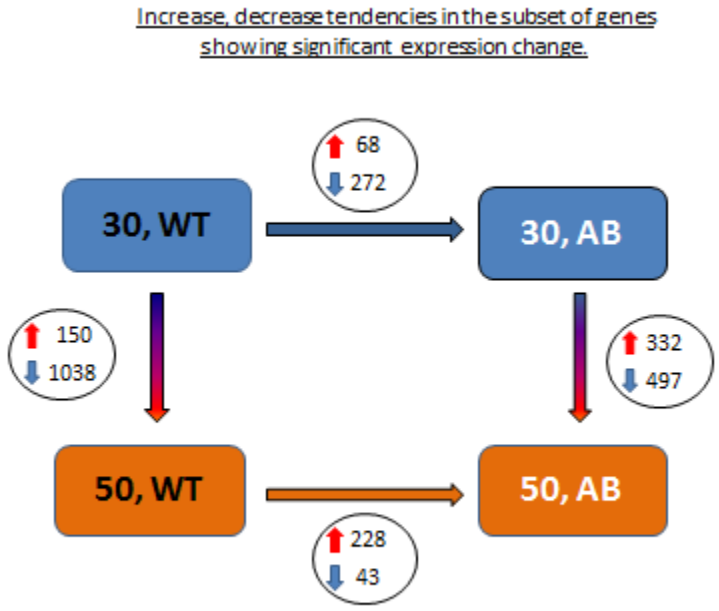

***Figure 5**. High throughput transcriptome analysis: Significant changes in the expression rates*

The IbpAB deletion caused changes in the mRNA level of several genes even under normal growth conditions (Fig.5). Interestingly, 272 genes showed downregulation in the mutant and most of them are involved in the metabolic processes (glycolysis, carbohydrate catabolism, cellular respiration, etc.). Only 68 genes showed elevated expression: those which are highly induced are coupled to the nucleotide (mainly purine) biosynthesis. Heat shock led to the repression of 1038 genes in wt cells particularly of those involved in the translation, as expected.

The same treatment resulted in the downregulation of only 497, mainly metabolic genes in IbpAB$^-$ cells. Only 150 genes were highly inducible in wt cells while 332 showed significant increase in the IbpAB$^-$ mutant. The genes involved in the response to the temperature and abiotic stress can be found on the top of the list in both cells. In general, we can conclude that deletion of the *ibpAB* operon has an unexpected pleiotropic effect on the whole transcriptome.

Regarding the genes involved in the fatty acid metabolism, heat shock decreased their overall expression in both strains. We could not find any significant difference between wild type and mutant which could be directly coupled to the alterations of fatty acid composition. Among the membrane-related genes, *envY* shows one of the highest alterations in mRNA level. It is induced by 140-fold in wt cells upon heat stress, but remains uninduced in the IbpAB$^-$mutant. The gene has a transcriptional regulatory effect on membrane pore forming genes (e.g. *ompC*, *ompF*). Interestingly, the expression of these target genes did not reflect the difference of the regulator. The intensity of expression changes of *rpoH* gene in the IbpAB$^-$ mutant is one of the most intriguing finding. This gene codes for a sigma factor (σ^{32}) which is the main transcriptional regulator of the heat shock genes in *E. coli*. As a feasible consequence, the mRNA levels of several genes -which are known to be controlled by *rpoH*-, have changed significantly in the IbpAB mutant. Since number of affected genes is high, it is very difficult to point which of them (probably more than one) can be responsible for the elevated thermotolerance of the IbpAB$^-$ mutant. Moreover, there are genes -whose expression levels are changed significantly- without known physiological functions. They might also play an important role in generating the observed phenotypical differences.

In summary, it has been demonstrated that deletion of the sHSP chaperones in *E. coli* resulted in very complex changes of the transcriptome. This might indicate, that besides their known membrane and protein defending functions sHSPs likely play other, hitherto unknown role(s) in the regulation of the whole cell metabolism. Such a prediction can well explain those of seemingly AB protein independent changes we have documented above. These include **unique fatty acid changes and fluidization in the hydrophobic core of the membranes, which are known to be associated with better survival upon heat challenge**.

CONCLUSION:

1. IbpAB proteins interact with membranes *in vivo* and *in vitro* and rigidify the membrane peripherial region. AB are localized to the heat-shocked *E.coli* membranes and counterbalance

heat-induced fluidization, indicating a direct protective, stabilizing role of AB in the heat-shocked membrane.

2. AB deficient cells have an increased membrane permeability but higher OM transition temperature and better survival at heat challenge.

3. An improved survival is linked to the altered membrane phenotype. These include unique fatty acid changes and fluidization in the hydrophobic core of the membranes. Altogether, AB proteins have a beneficial role in the membranes upon heat.

4**.** A specific and indispensable role for AB proteins could be of preserving and aiding recovery of heat denatured membrane proteins after stress. (This is in good agreement with the proposed role of AB proteins in the soluble fraction.)

II. *Synechocystis* DnaK2 chaperone-thylakoid structure-function connection

Our present hypothesis is, that the specific, lipid-mediated membrane association of Hsps in *Synechocystis* is not confined for cyanobacterial Hsp17 and GroEL(S) but it is also a feature of additional stress protein chaperone, DnaK, a homolog of mammalian Hsp70. Here we show, that being either "resident" or "visitor" (i.e. located within or on the surface of membranes) on membranous organelles, a specific subset of DnaK2 may participate in those homeostatic controlling mechanisms, which ultimately retailor the lipid composition and membrane physical-chemical state and consequently the basic functions of Hsp-hosting membranes.

We proved already that in *Synechocystis* PCC6803 there are 3 DnaK family members (which belong to Hsp70 chaperone family). Out of these 3 DnaKs, one, DnaK2 is transcriptionally active and more importantly, its protein level is temperatutre inducible. We identified the gene product protein by Western blot and found, that this Hsp is localized mainly to the cytoplasm, but a subset is thylakoid associated.This observation suggests the notion, that DnaK2 might have a membrane protective role under normal conditions which becomes more effective when cells were subjected to heat stress.

Our aim was to address the following questions:

1. is there an interaction between DnaK2 and any of *Synechocystis* lipid classes,

2. is DnaK2 important in thylakoid stress management and whether DnaK2 deletion will affect the cellular stress tolerance, especially of the photosynthesis,

3. does such a mutation affect the physico-chemical properties (fluidity) of the thylakoids

4. will a partial lack of DnaK2 affect lipid composition of the thylakoid membranes.

1.Interacation between DnaK2 and monolayers made of *Synechocystis* lipids

Expression and purification of Synechocystyis DnaK2 protein.

E.coli BL21 Codon + RIL was transformed with pET24a(+) vector containing DnaK2 coding sequence. The transformed cells were cultured in Lauria-Bertani medium (containing 25 µg/ml kanamycin) at 37°C on a platform shaker (220 rpm). Protein expression was induced with 1 mM IPTG. The harvested cells (around 0.4 g bacteria) were disrupted by sonication. The suspension of disrupted cells was centrifuged at 18,000g for 30 min at 4°C. The supernatant was applied on HITrap Q (GE Healtcare) column with 0.2 – 0.4 M NaCl linear gradient. To the fraction containing Dnak2 was added 5 mM MgCl2 and incubated for 4 hours at 4°C with 3 ml ATP agarose (SIGMA). The Dnak2 protein was eluted with 25 mM ATP (Fig.6). Protein concentration was determined by the micro BCA method.

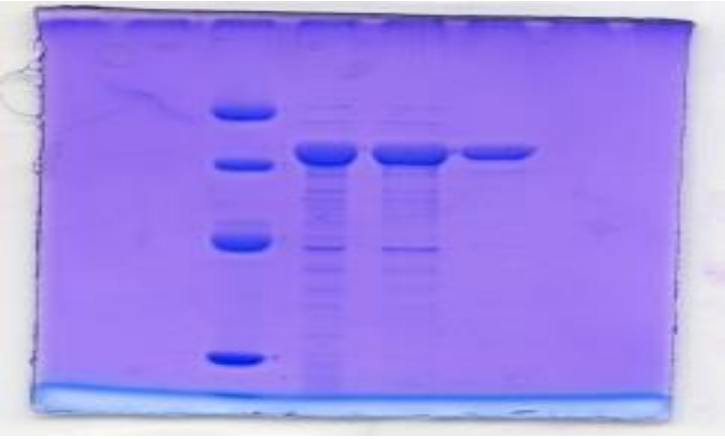

Figure 6. *12% SPS-PAGE of purified DnaK2 protein*

Lipid extraction and separation of lipid classes by thin layer chromatography

For lipid isolation and analysis, *Synechocystis sp*. PPC 6803 were cultured to 1.6 OD_{800} unit/mL (total 1500 mL), washed and resuspended in H_2O. Lipids were extracted according to a modified Folch procedure and dissolved in chloroform:methanol (2:1, by vol.). To isolate the total polar lipid (TPL) fraction for monolayer experiments, the total lipid extract was separated on Kieselgel 60 silica gel TLC plates (20x20 cm, Merck, Germany, Darmstadt). The TPL fraction was scraped off, washed three times and resuspended in chloroform:methanol (2:1, by vol.).

The isolation of major polar lipid classes (sulfoquinosyldiacylglycerol (SQDG), monogalactosyldiacylglycerol (MGDG), digalactosyldiacylglycerol (DGDG) and phosphatidylglycerol (PG)) was carried out from total polar lipid extract. To quantify these lipids, a known amount of C15:0 free fatty acid was added as an internal standard for the visualized spots on TLC. The spots were scraped and the scrapings were directly methylated in 5 % acetyl chloride in methanol at 80 °C for 2 h. The resulting fatty acid methyl esters (FAMEs) were extracted with hexane, the solvent was evaporated and the residue redissolved in 50 µL benzene and analysed by MS-coupled gas chromatography.

Monolayer Experiments

Interaction of DnaK2 with monomolecular lipid layers was measured using a KSV3000 Langmuir Blodget instrument (KSV Instruments, Helsinki). Briefly, isolated lipids dissolved in chloroform/methanol directly spread onto the surface of sodium phosphate buffer, pH 7.2 at

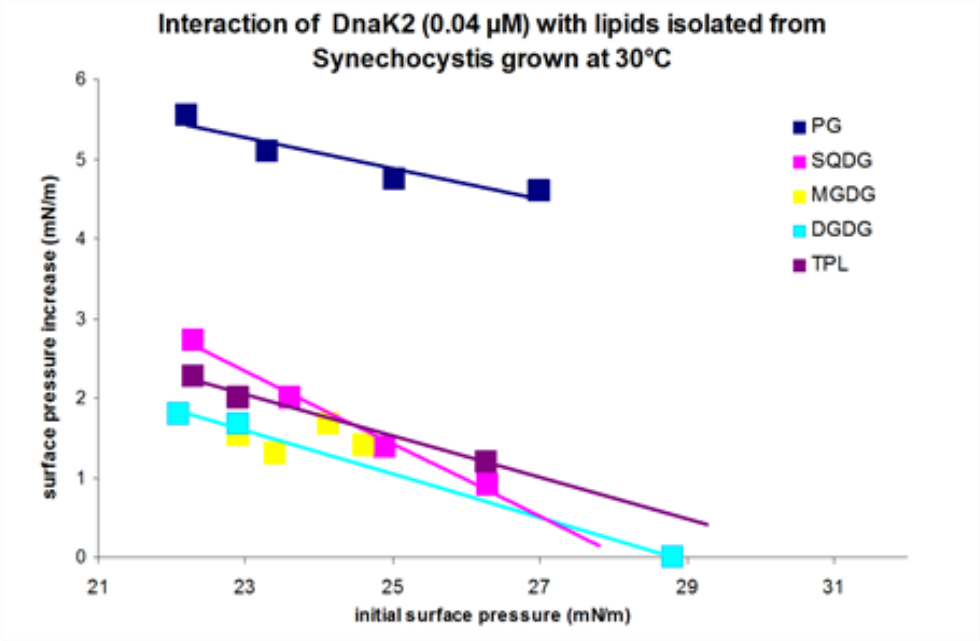

Figure 7*. Monolayer experiment. Interacation of DnaK2 with different lipids isolated from Synechocystis*

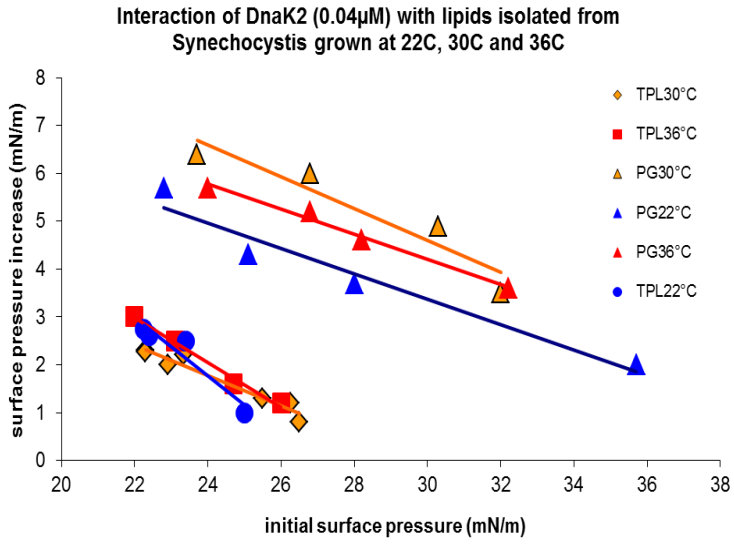

Figure 8. *Monolayer experiment. Interaction of DnaK2 with TPL and PG isolated from cells grown at different temperatures*

room temperature formed different initial surface pressure. The purified DnaK2 protein was injected (0.4μM) underneath the monolayers and the subsequent changes in surface pressure were determined (Fig.7).

Fig.7 shows that although all isolated lipid classes are able to interact to some extent with DnaK2, however the interaction was far more higher with phosphatidyl glycerol (PG) than with any other lipids. This is a very important finding, as it is known that *Synechocystis*, defective for the biosynthesis of PG, requires PG supplementation for growth. It is also documented that PG contributes to the accumulation of chlorophyll–protein complexes in thylakoid membranes, and also to normal functioning of PSII. More precisely it was shown that PG plays an important role in binding extrinsic proteins required for sustaining a functional Mn cluster on the donor side of PSII. It is intrigiung to suppose that DnaK2 binds to regions of thylakoid membrane where PSII complex is assembled to help this assembly. Such an association of DnaK2 may take place trough binding of DnaK2 specifically to PG. It is important to mention, that the binding is influenced to some extent by the temperature at which the *Synechocystis* was grown (Fig.8).

To find the reason, we determined the fatty acid composition of PG isolated from cells grown either at 30 or 22 °. As Table 2. shows, there is a very pronounced difference in the fatty acid composition, namely PG isolated from cells grown at lower tempetrature (22 °C) is much more unsaturated (containing much higher amount of 18:3 fatty acid) than PG isolated from cells grown at 30 °C. This difference in fatty acid composition could well explain the difference in DnaK2 binding.

Growth temperature	**16:0**	**16:1**	**18:0**	**18:1**	**18:2**	**γ18:3**	**α18:3**
22 °C	52.1	0.9	1.9	4.3	22.2	1.1	17.4
30 °C	64.6	1.0	3.9	5.8	22.6	0.8	1.3

Table 2*. Fatty acid composition of PG isolated from cells grown either at 22 or 30 °C. Data are shown as % of the total fatty acids*

2.Photosynthetic characterization of *Synechocystis PCC 6803 dnaK2* mutant.

Backgound

Photosystem II (PSII) of the photosynthetic apparatus is a multi-subunit pigment-protein complex in the thylakoid membrane, which performs light-induced oxidation of water and reduction of plastoquinone. During light energy conversion the PSII complex suffers photo-oxidative damage, which is induced by both the visible and UV-B part of the solar spectrum, which target primarily the Mn cluster of the water-oxidizing complex in PSII and leads to damage and subsequent degradation of D1 and D2 reaction center subunits.

Photodamage, induced either by visible or UV-B ligth can be restored via protein synthesis dependent repair. The most important step in the repair is the *de novo* synthesis of photodamaged D1 and D2 subunits of the PSII reaction center. The key step of the repair process is the degradation of damaged D1 and D2 subunits by the FtsH protease, followed by *de novo* synthesis and reinsertion of D1 into the PSII complex. However, this process involves a number of other proteins, as well. In light of our above findings we speculated, that such possible candidates are the DnaK-type proteins, encoded by the *dnaK-type* genes, whose amount is increasing under heat- as well as light-stress.

In order to obtain better insight into the potential role of DnaK-type proteins in PSII repair we studied mutants of the cyanobacterium *Synechocystis* PCC 6803, which lack the majority of the *dnak2* gene and is unable to produce the respective protein. Since DnaK2 turned out to be essential for *Synechocystis* cells the *dnak2* gene could not be fully eliminated, and the mutant cells contained different portions of the gene. Hence we worked with three different clones of the dnaK2 mutant, out of which clone-1 has the lowest level of dnaK2 mRNA.

Effect of Δdnak2 mutation on PSII repair assessed by O_2 evolution rate measurements

In order to assess the electron transport characteristics and light tolerance of these clones, we applied flash-induced fluorescence relaxation and oxygen evolution measurements.

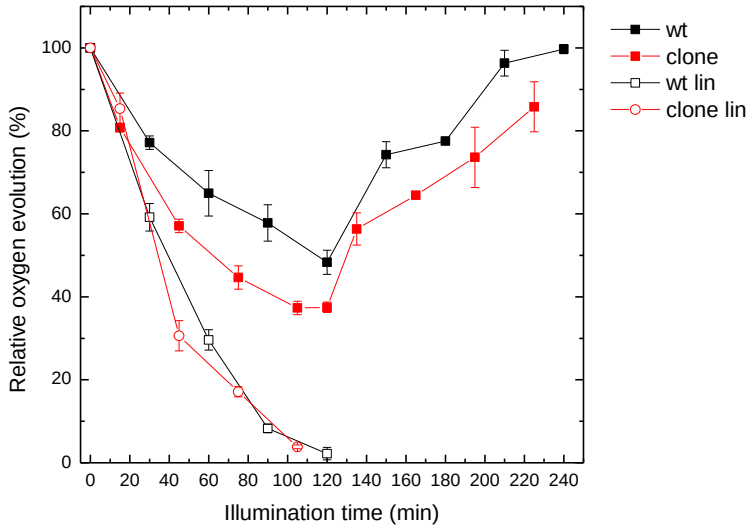

Figure 9. *Effect of UV-B/low light illumination on the rate of oxygen evolution in wild type (black squares) and Ddnak2 clone 1 (red squares) cells without addition, or in the presence of 300 mg/ml lincomycin (open symbols) of Cells grown at 30 °C, and 40 µmol m^{-2} s^{-1} light intensity were subjected to 10 µmol m^{-2} s^{-1} UV-B light for 2 h, followed by 2 h recovery period under growth light.*

Measurement of oxygen evolution rate is an effective method to observe both the damage and the repair of the PSII complex. Our data show that exposure to UV-B radiation induced larger loss of PSII activity in the mutant, which lacks most of dnaK2, than in the WT (Fig.9). However, when the UV-B treatment was performed in the presence of the protein synthesis inhibitor, lincomycin the WT and Δdnak2 cells were damaged to the same extent (Fig. 9). Based on these data we can conclude that in the absence of the DnaK2 protein, the sensitivity of the PSII against UV-B radiation is increased due to partial inhibition of PSII repair. This effect may result from the direct involvement of the DnaK2 in the PSII repair cycle, or can occur as a consequence of changes induced by the absence of DnaK2 in membrane composition, which leads to increased membrane rigidity (see later).

Effect of Δdnak2 mutation on PSII electron transport

In order to determine if the presence or absence of the DnaK protein has any effect on the electron transport characteristics of PSII, we monitored forward and reverse electron flow by using chlorophyll fluorescence relaxation kinetic measurements:

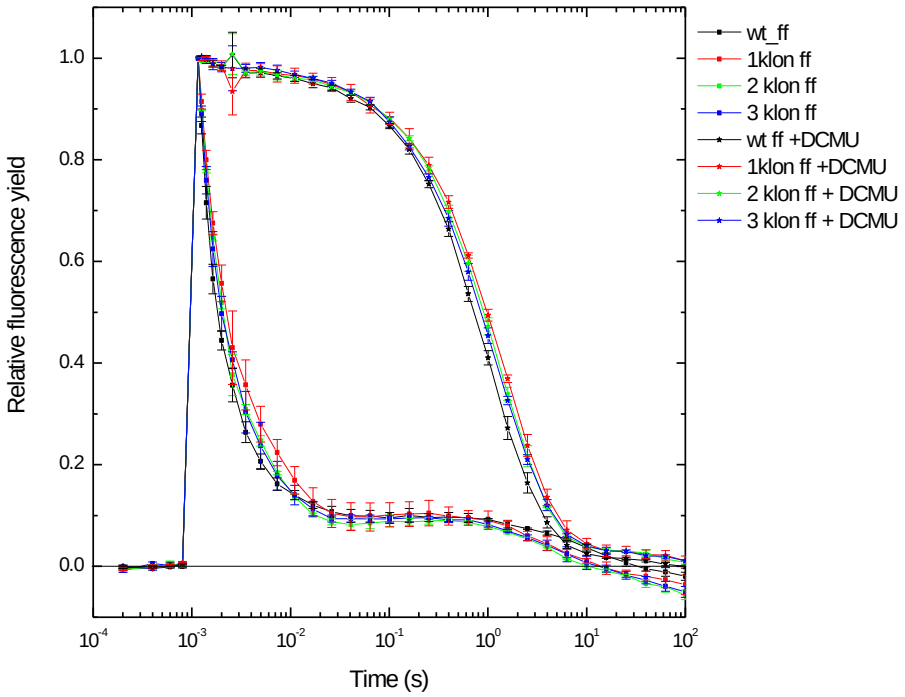

Figure 10. *Flash-induced fluorescence decay in wild type (black), Δdnak2 clone 1 (red), Δdnak2 clone 2 (green) and Δdnak2 clone 3 (blue) cells in the absence (closed symbols) and in the presence of 10 μM DCMU (open symbols).*

In the absence of electron transport inhibitor the fluorescence relaxation shows a 3-phase kinetics (closed symbols in Fig10). The fast phase (450-550 μs) reflects electron transfer from the Q_A to the Q_B plastoquinone electron acceptor, which is a PQ molecule occupying the Q_B plastoquinone-binding site. The middle phase (3-4 ms) also arises from electron transfer from Q_A to Q_B, but in such PSII centers that bind PQ molecules after the light pulse, *i.e.* the time constant of this phase shows the rate of PQ binding to the Q_B site. Finally the slow phase (a few seconds) arises from backward electron transport from Q_B to the oxidized *S*2 state of the water-oxidizing complex. In the presence of DCMU, which blocks forward electron transport from Q_A^- to Q_B, Q_A^- reoxidation proceeds via charge recombination with the S2 state of the water oxidizing complex (ca. 1s).

Flash-induced fluorescence measurements showed that forward electron transport between Q_A^- and Q_B is slower in the ΔdnaK2 cells that in the WT (Fig. 10, Table 3), which indicates a direct, or indirect effect of the DnaK2 protein on PSII electron transport.

	amplitude %	fast phase t1/2 µs	amplitude %	middle phase t1/2 ms	amplitude %	slow phase t1/2 s
WT	52.3	440.8	30.9	3.3	16.8	4.5
1 klon	44	530.6	40.6	4	15.4	2.3
WT+DCMU	0.12	50			99.88	0.8
1 klon+DCMU	0.09	137			99.91	1.1

Table 3*. Amplitudes and half life-times of Chl fluorescence relaxation components in WT and ΔdnaK2 mutant cells.*

Effect of Δdnak2 mutation on PSII repair assessed by Chl fluorescence relaxation measurements

Chl fluorescence relaxation measurements provide information not only on the characteristics of PSII electron transport, which can be deduced from the decay kinetics, but also on the amount of functional PSII centers, which can be deduced from the initial fluorescence amplitudes. The initial fluorescence amplitudes are decreasing in a parallel fashion in the different Δdnak2 mutant lines during UV-B exposure in the presence of the protein synthesis inhibitor lincomycin.

However, the WT cells show a faster amplitude loss (Fig.11. open symbols). Also, in the absence of lincomycin the WT cells show faster loss of initial fluorescence amplitude than the Δdnak2 mutant lines. These data show an opposite tendency than obtained from the oxygen evolution data (Fig. 9). In principle, the rate of oxygen evolution reflects the capacity of the PS complex to produce O_2, while the fluorescence amplitude shows the number of the functional PSII complexes, which are capable of charge separation in PSII. However, in case of Chl fluorescence various quenching mechanisms may also influence the fluorescence amplitude. To explain the different behavior of UV-B induced loss of O_2 evolving capacity and of fluorescence amplitude we assume that the absence of the DnaK2 protein may influence the efficiency of fluorescence quenching in *Synechocystis* cells. This effect is most probably an indirect consequence of the lack of DnaK2 on the structure of the thylakoid membrane.

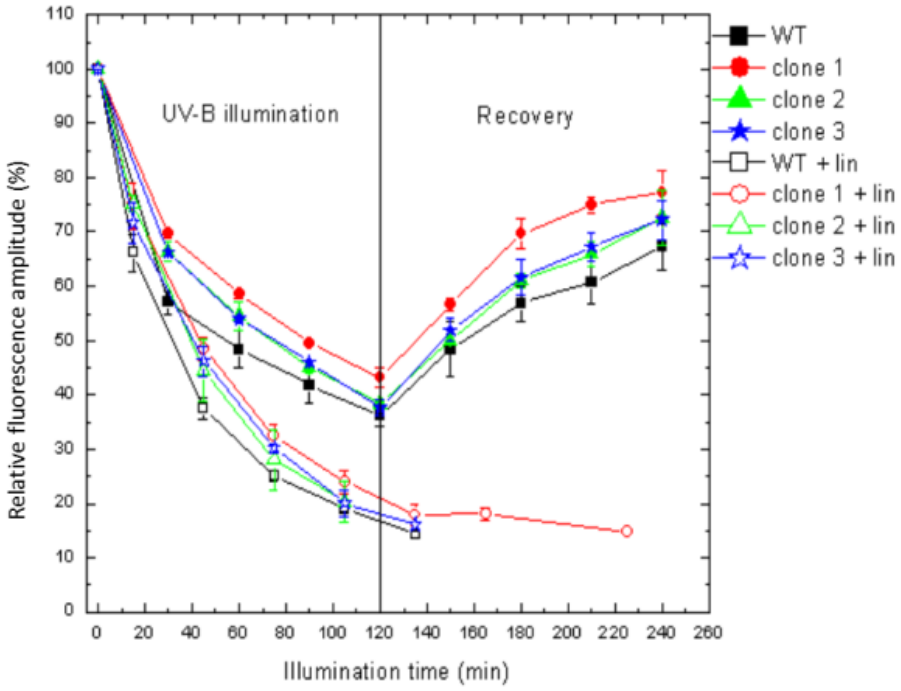

Figure 11. *Effect of UV-B/low light illumination on the initial amplitudes of flash-induced fluorescence decay in wild type (squares), Δdnak2 clone 1 (circles), Δdnak2 clone 2 (triangles) and Δdnak2 clone 3 (stars) mutants and in the presence (open symbols) of 300 mg/ml lincomycin. Cells grown at 40 µmol* m^{-2} s^{-1} *were subjected to 10 µmol* m^{-2} s^{-1} *UV-B light for 2 h, followed by 2 h recovery period under growth light.*

Effect of growth temperature on the influence of the ΔdnaK2 mutation on PSII recovery

Since the DnaK2 protein can be induced by heat treatment of *Synechocystis* cells we also wanted to check if growth temperature of cells has any influence on the effect ΔdnaK2 mutation on PSII repair, or not? According to the data shown in Fig. 12. when cells were grown at 30 °C, but the UV-B treatment was performed at 36 °C, the ΔdnaK2 mutant strain lost its O_2 evolving activity during UV-B treatment with same kinetics as the WT strain.

This effect supports the hypothesis that lack of the DnaK2 protein modifies the membrane structure and induces its higher rigidity at the growth temperature of the cells. However, this effect can be compensated by the increased temperature of the measurements, which leads to increased fluidity of the membrane.

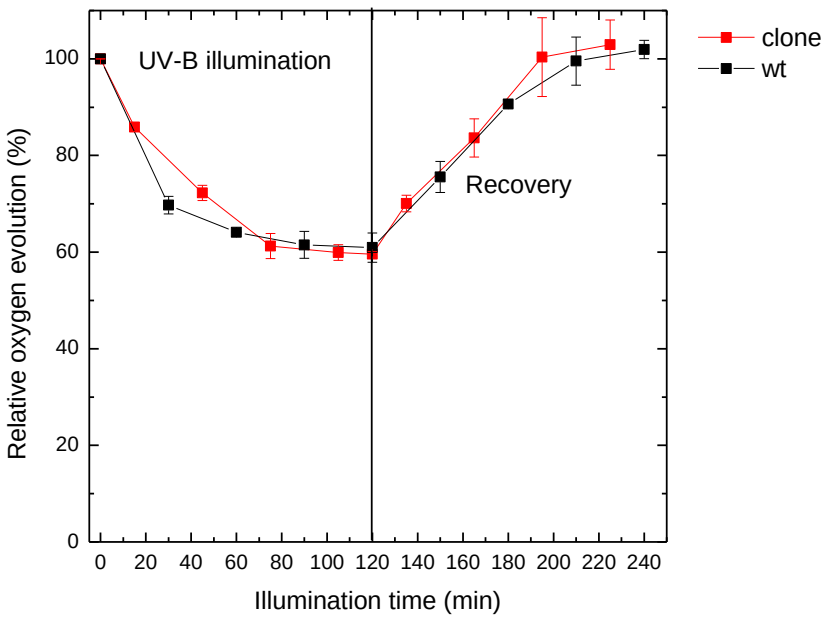

Figure 12. *Effect of UV-B/low light illumination on the oxygen evolution in wild type (black squares) and ΔdnaK2 clone 1 (red squares) mutant. Cells grown at 30 °C, with air bubbles, 40 µmol* m^{-2} s^{-1} *were subjected to 10 µmol* m^{-2} s^{-1} *UV-B light for 2 h, followed by 2 h recovery period under growth light, in 36* °C.

We can **conclude**, that the lack of the DnaK2 protein leads to the partial inhibition of PSII repair at the growth temperature of the cells. In addition the rate of forward electron transport between the Q_A and Q_B quinone electron acceptors is slowed down.

These data indicate that the DnaK2 protein interacts with the tylakoid membrane and/or with the PSII complex. This interaction leads directly or indirectly to changes in membrane fluidity (increased rigidity at growth temperature), which influences PSII repair and PSII electron transport, as well.

3. The aim of the next experiments was to **determine the temperature dependent changes of the thylakoid membrane fluidity** of wild type (WT) and DnaK2 mutant cells.. We have shown, that the thylakoid membrane derived from the mutant cells is generally more ordered than the

wild type membrane (30 dnaK2- vs. 30 WT and 44 dnaK2- vs. 44WT). It is noted that both strains retained their capacity to elevate membrane order upon heat adaptation (Fig.13).

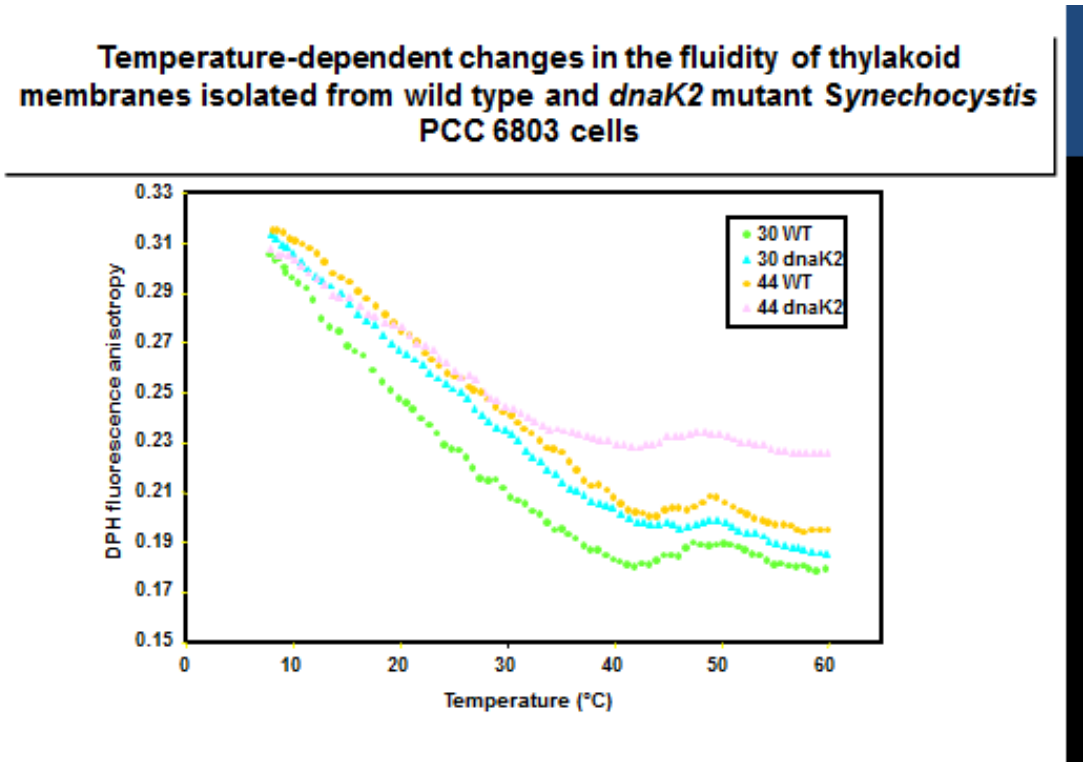

Figure 13. *Temperature dependent changes in the fluidityof WT and mutant starin*

4. Very surprisingly, the reduction of DnaK2 level also influenced the **fatty acid composition** of membranes, as tested in total lipids. A significant (two-fold) increase in the amount of oleic acid (18:1) on the expense of polyunsaturated fatty acids (18:2, 18:3) was observed in the case of mutant cells in comparison to its WT counterpart (Table 4.).

Strains	**16:0**	**16:1**	**18:0**	**18:1**	**18:2**	**γ18:3**	**α18:3**
WT	49.8	4.8	1.1	**5.9**	16.2	21.7	0.4
ΔDnaK2	50.6	4.5	1.3	**12.9**	12.7	17.5	0.5

Table 4. *Effect of reduced DnaK2 protein level on the fatty acid composition of total lipids of thylakoid membrane preparations. Numbers are expressed as % of total fatty acids*

Taken together: the primary composition and physical state of the lipid phase of membranes can control both the expression and membrane-association of pre-existing Hsps at the early phase of heat stress. Interaction of newly formed Hsps with membranes (together with a hitherto unexplored cross-talk of stress protein and membrane lipid homeostasis) may represent an additional layer of this control. In case of having more experimental support of the above predictions, our findings will urge a substantial reevaluation of the basic cellular functions ascribed to the stress protein molecular chaperones.